Title

Unravelling the neural dynamics of hypnotic susceptibility: Aperiodic neural activity as a central feature of hypnosis

Authors

Mathieu Landry[1], Jason da Silva Castanheira[2], Catherine Boisvert[3], Floriane Rousseaux[4], Jérôme Sackur[5], Amir Raz[6], Philippe Richebé[4,7], David Ogez[4,7], Pierre Rainville[8,9], Karim Jerbi[1,10,11]

Affiliations

[1] Département de Psychologie, Université de Montréal, Montreal, Qc, Canada

[2] Montreal Neurological Institute, McGill University, Montreal, Qc, Canada

[3] Département de Neurosciences, Université de Montréal, Montreal, Qc, Canada

[4] Centre de Recherche Hôpital Maisonneuve-Rosemont, Montreal, Qc, Canada

[5] Laboratoire de Sciences Cognitives et Psycholinguistique, ENS, PSL University, EHESS, CNRS, Paris, France

[6]Institute for Interdisciplinary Behavioral and Brain Sciences, Chapman University, Irvine, CA, USA. 92618.

[7] Département d'Anesthésiologie et de Médecine de la douleur, Université de Montréal, Montreal, Qc, Canada

[8] Départment de Stomatologie, Faculté de Médecine Dentaire, Université de Montréal, Montréal, Canada

[9] Centre de Recherche de l'Institut Universitaire de Gériatrie de Montréal (CRIUGM), Université de Montréal, Montréal, Canada

[10] MILA - Quebec Artificial Intelligence Institute, Montreal, Qc, Canada

[11] UNIQUE Center (Quebec Neuro-AI Research Center), Montreal, Qc, Canada

Corresponding author: Mathieu Landry (mathieu.landry@umontreal.ca)

Abstract: 170 words
Body: 5196 words

Key Words

Hypnosis, Resting-State EEG, Spectral Analysis, Aperiodic Activity, Connectivity, Machine Learning, Altered State of Consciousness, Classification

Acknowledgments
M.L. acknowledges support from the Fonds de Recherche du Québec – Nature et Technologies, the Natural Science and Engineering Research Council of Canada. M.L., J.S. and A.R. acknowledge support from the Bial Foundation (Grant #280/16). J.d.C. acknowledges support from the Natural Science and Engineering Research Council of Canada. M.L., D.O. P.R. and K.J acknowledges support from the Fonds de Recherche du Québec – programme Audace (337355). K.J. is supported by funding from the Canada Research Chairs (950-232368) program and a Discovery Grant from the Natural Sciences and Engineering Research Council of Canada (2021-03426). We would also like to thank members of the HyMed lab and CoCo Lab.

Contributions
Designed Research: All authors. Performed Research: M.L. and J.d.C. Funding acquisition: M.L., J.S., A.R., D.O., P.R. K.J. Contributed new analytic tools: M.L. and J.d.C. Analyzed Data: M.L. and J.d.C.; Wrote the Paper: All authors.

Competing Interests
All authors declare no competing interest.

Data availability
Data for the analyses supporting the current study is publicly available on the Open Science Framework repository:

Code Availability
Code for the analyses supporting the current study is publicly available on the Open Science Framework repository:

Abstract
How well a person responds to hypnosis is a stable trait, which exhibits considerable inter-individual diversity across the general population. Yet, its neural underpinning remains elusive. Here, we address this gap by combining EEG data, multivariate statistics, and machine learning in order to identify brain patterns that differentiate between individuals high and low in susceptibility to hypnosis. In particular, we computed the periodic and aperiodic components of the EEG power spectrum, as well as graph theoretical measures derived from functional connectivity, from data acquired at rest (pre-induction) and under hypnosis (post-induction). We found that the 1/f slope of the EEG spectrum at rest was the best predictor of hypnotic susceptibility. Our findings support the idea that hypnotic susceptibility is a trait linked to the balance of cortical excitation and inhibition at baseline and offers novel perspectives on the neural foundations of hypnotic susceptibility. Future work can explore the contribution of background 1/f activity as a novel target to distinguish the responsiveness of individuals to hypnosis at baseline in the clinic.

Significance Statement
Hypnotic phenomena reflect the ability to alter one's subjective experiences based on targeted verbal suggestions. This ability varies greatly in the population. The brain correlates to explain this variability remain elusive. Addressing this gap, our study employs machine learning to predict hypnotic susceptibility. By recording electroencephalography (EEG) before and after a hypnotic induction and analyzing diverse neurophysiological features, we were able to determine that several features differentiate between high and low hypnotic susceptible individuals both at baseline and during hypnosis. Our analysis revealed that the paramount discriminative feature is non-oscillatory EEG activity before the induction—a new finding in the field. This outcome aligns with the idea that hypnotic susceptibility represents a latent trait observable through a plain five-minutes resting-state EEG.

Introduction

Hypnosis modifies sensory perception, cognitive abilities, ideomotor actions, and emotional responses by targeted manipulation of the brain's top-down mental processes through hypnotic suggestions. (1). This response is often characterized by changes in phenomenology, including sensations of profound relaxation, heightened mental absorption, and shifts in volitional control (2-4) which are often construed as a defining feature of hypnotic phenomena (5). In this way, hypnosis encompasses the directed modulation of information processing in a manner that aligns with the content of hypnotic suggestions (e.g., altering the neural representation and interpretation of nociceptive signals in the context hypnotic analgesia; 6), and the spontaneous alterations across diverse phenomenological dimensions (e.g., 7). Hypnotic phenomena are therefore multifaceted and hardly reducible to a single dimension or feature.

The scientific landscape of hypnosis is marked by intricate complexity involving several hypotheses, methodologies, and interpretive frameworks (8). This heterogeneity includes studies investigating the neurophenomenological facets of hypnosis (e.g., 9), alongside those aiming to uncover the neural underpinnings of hypnotic responsiveness (e.g., 10). The primary consequence of this heterogeneity is that the resulting body of research exhibits a wide diversity of findings (11-13), including results about susceptibility to hypnosis (14, 15). Within the experimental context of electrophysiological recordings, research shows that multiple aspects of the signal relate to hypnotic phenomena. These findings encompass modulations of spectral power (16), evoked responses (e.g., 17), the fractal component of the electroencephalographic signal (18), shifts in connectivity patterns (e.g., 19), as well as changes in the intricate organization of network topology (20). Previous research highlights the contribution of multiple broad bands of the EEG signal (e.g., theta band activity; 21). Likewise, neuroimaging studies link hypnotic phenomena to diverse brain regions, including alterations in the interplay among resting-state networks—such as the central executive, the salience, and the default networks(11). This wide variety of findings in the literature reflects the inherent complexity of hypnosis and demonstrates the multi-faceted nature of hypnotic responding (22). Taken together, the existing body of work not only highlights the diverse methodologies and perspectives employed to probe hypnosis but also points to the intricate relationship between hypnotic phenomena and various underlying cognitive and neural mechanisms (23).

To tackle the inherent complexity of hypnotic phenomena at the brain level, neuroscientific research largely centers on the exploration of three key variables: Susceptibility to hypnotic suggestions, the induction procedure, and the impact of suggestions (24). The susceptibility to hypnotic suggestions refers to a stable psychological trait that primarily signifies the ability to effectively respond to direct verbal suggestions within controlled and standardized settings (25). Notably, susceptibility to hypnotic suggestions serves as a predictive indicator across both experimental and clinical contexts of hypnosis (26). Inter-individual differences therefore represent a pervasive aspect of hypnotic responding that may challenge the broad implementation of clinical hypnosis. Consequently, it is crucial to deepen our understanding of this specific aspect to enhance the effectiveness and applicability of hypnotherapy. In turn, the induction procedure constitutes an integral part of most hypnotic protocols (27).

Our work builds upon previous EEG-based research and determines the contributions of oscillatory (periodic) and non-oscillatory (aperiodic) components of the power spectrum to hypnotic susceptibility. The aperiodic component of the neural power spectrum corresponds to scale-free background activity that approximates a power-law distribution ($P \propto 1/f^{\beta}$), whereas the periodic component denotes discernible peaks in the frequency domain (28, 29). Both the aperiodic and periodic elements of the power spectrum hold relevance across a wide range of psychological phenomena, spanning sensations and cognition, developmental trajectories and aging, as well as clinical and pharmacologically-induced mental states, and altered states of consciousness (30-35).

Furthermore, given that hypnosis is thought to influence the efficiency of brain networks, we relied on a graph theoretical approach to understand how brain networks relate to hypnotic susceptibility (36). Indeed, a recent EEG study employed graph theory to show that the hypnotic induction increases brain networks in HHSIs segregation in delta and alpha bands, and integration in the beta-band (20). Accordingly, the hypnotic procedure reconfigures functional brain networks both at local and global levels. The present work therefore focused on these topological aspects of EEG.

The primary objective of the current study is to elucidate the underlying neural dynamics associated with susceptibility to hypnosis before and after a hypnotic induction. We accomplish this through the integration of high-density electroencephalography (EEG), advanced multivariate pattern classification techniques, and machine learning methodologies. We accordingly aimed to assess which neural features could be used to discriminate between individuals with high (HHSIs) and low hypnotic susceptibility (LHSIs) both at baseline--prior to the hypnotic induction--and based on the hypnotic effect (post- minus pre-induction: Δinduction; **Figure 1**). We hypothesize that numerous neural attributes inherent to EEG exhibit direct relevance to our focal variables. Furthermore, given that susceptibility to hypnosis represents a stable trait, we expect that these attributes will be present for both prior to induction (i.e., pre-induction) and after hypnotic induction (Δinduction).

Results

We discriminated between and high and low hypnotic susceptible individuals using a linear support vector machine (SVM) with a leave-one-out cross validation procedure (**Figure 1C**). We first tested the classifier's discrimination ability based on spectral features. These features included rhythmic activity across delta (1 to 3.5Hz), theta (4 to 7.5Hz), alpha (8 to 13.5Hz), and beta (14 to 39Hz) frequencies, as well as the aperiodic offset and exponent values from estimates of non-oscillatory activity (**Figure 1A**). See Methods for details.

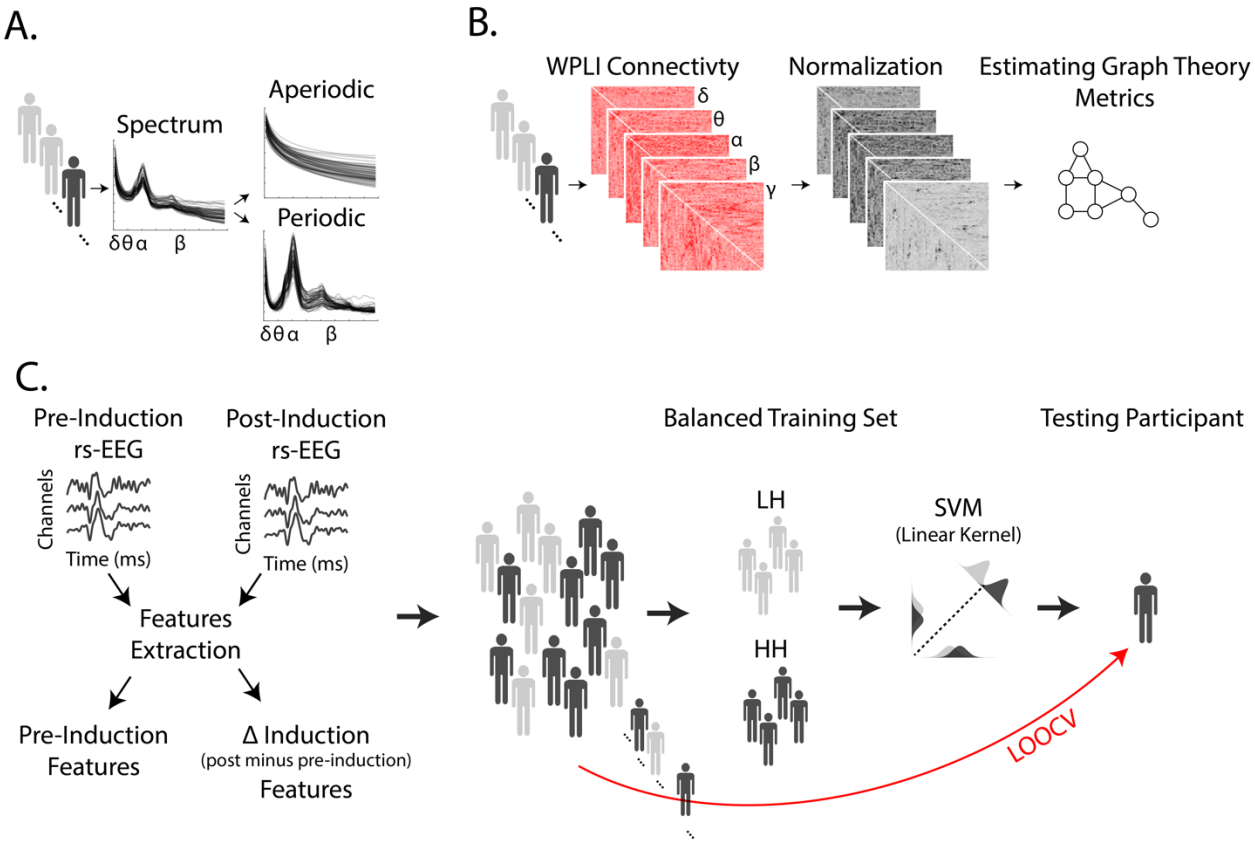

Figure 1. Analysis pipeline for extracting power spectrum and network topology features and performing multivariate pattern analysis with leave-one-out cross-validation. **A.** Aperiodic and periodic components of the power spectrum were estimated for each participant using 5 minutes of eye-closed rs-EEG data, both pre- and Δinduction. **B.** Connectivity patterns between EEG channels were calculated using weighted Phase Lag Index (wPLI) across delta, theta, alpha, beta, and gamma frequencies. The connectivity matrices were normalized from 0 to 1 (37). Clustering coefficient, global efficiency, and modularity were computed using graph theory for each network. **C.** High and low hypnotic susceptible individuals were classified based on these metrics using multivariate pattern analysis with leave-one-out cross-validation (LOOCV) employing linear Support Vector Machine (SVM). EEG channels were included as features of this linear model. Each training iteration included balanced classes of low (light grey) and high (dark grey) hypnotic susceptible individuals, while one participant was left out for validation.

Spectral features. For the pre-induction period, our SVM classification yielded statistically significant results for the aperiodic exponent (**Figure 2A**; AUC = .69, $p < .001$). However, classification performance based on other spectral features, including oscillatory activity, did not reach significance (**Figure 2A**). We conducted further analysis to examine the weights of the classifiers, which provided insights into the specific contributions of the topographical features (**Figure 2A).** Notably, we observed a widespread neural pattern indicating that high hypnotic susceptible individuals exhibit a greater aperiodic exponent across the entire scalp. However, this pattern was particularly pronounced in the anterior part of the frontal site (**Figure 2A**; with the highest averaged coefficient value observed at channel AF8) and the right temporal region. We note that we did not observe any difference in aperiodic exponents between LHSIs and HHSIs for Δinduction (**Figure 1C**; **supplementary Figure 1C**). These findings highlight the importance of aperiodic activity

relative to hypnotic susceptibility, while the induction procedure does not alter this neural feature.

In contrast, periodic delta activity distinguished between LHSIs and HHSIs for Δinduction (**Figure 2C;** AUC = .57, p < .01). The corresponding topography highlights the frontal channels (**Figure 2C**). We note that during the post-induction, HHSIs and LHSIs exhibit similar delta power values, whereas HHSIs appear to show greater delta power value during pre-induction period (**supplementary Figure 1D-F**). Hence, our findings reveal that the induction has a greater impact on rhythmic delta band activity for HHSIs compared to LHSIs.

Note we assessed the contribution of ocular artifacts to participant classification by defining classifiers based on electro-oculogram signals. This analysis revealed we could not discriminate between HHSIs and LHSIs.

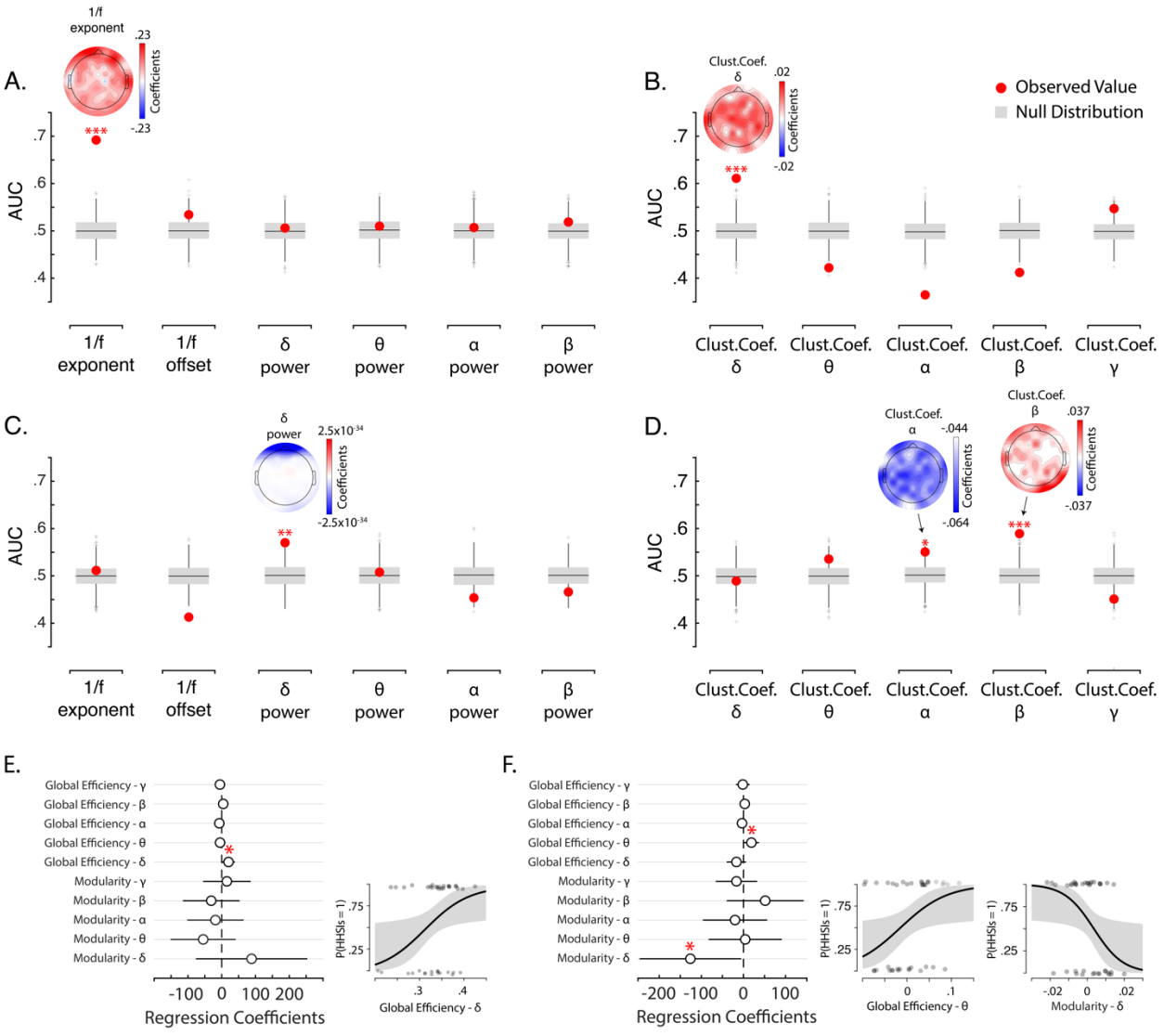

Figure 2. Panels A and B show analysis for pre-induction EEG, whereas panels C and D show analysis for Δinduction EEG. Panels A, B, C and D show AUC values for assessing classification performances of SVM linear models for accurately classifying high and low hypnotic susceptible individuals in LOOVC based on aperiodic and periodic features of the power spectrum during the EEG pre-induction period (A) and the Δinduction period (C), as well as graph theoretical clustering coefficients calculated from pairwise wPLI across frequency bands during the EEG pre-induction period (A) and for Δinduction (D). Red dots show observed AUC values. Boxplot shows surrogate null distributions based on random permutations where we shuffled the labels during training. The bottom and top whiskers indicate the first and third quartiles, respectively. Three asterisks indicate statistical significance at $p < .001$, two asterisks at $p < .01$, one asterisk at $p < .05$. Topographies show the averaged coefficient values of the SVM models from all iterations and LOOVC approach for the neural features that can discriminate high and low hypnotic susceptible individuals better than chance-level. Panel E shows the coefficient values and 95 C.I. from the logistic regression model assessing if global efficiency and modularity for pre-induction EEG across all frequency bands predict hypnotic susceptibility. Panel F show likelihood estimates for significant coefficients, global efficiency in the delta frequency band. Each dot represents individual data points and the grey area represents 95% C.I. The sigmoid function shows likelihood estimates for significant coefficients. Each dot represents individual data points, and the grey area represents 95% C.I. Red asterisks indicate significant coefficient at $p < .05$.

Network topology. We then evaluated the classifier's ability to discriminate between high and low hypnotic susceptible individuals based on graph theory clustering coefficients from channel-wise connectivity patterns as neural features (**Figure 1B**). Connectivity was estimated applying weighted Phase Lag Index (38) based on neural activity across delta (1 to 3.5Hz), theta (4 to 7.5Hz), alpha (8 to 13.5Hz), beta (14 to 39Hz), and gamma (30 to 50Hz) frequencies.

We first examined whether classifiers could distinguish between LHSIs and HHSIs individuals based on clustering coefficients. In the pre-induction EEG recording, we found that the classification performance was statistically significant for clustering coefficient in the delta frequencies (**Figure 2B**; AUC value = .61, $p < .001$). Analyzing the weights of the classifiers, we observed widespread higher clustering coefficients in high hypnotic susceptible individuals, slightly concentrated in the central and bilateral temporal regions (**Figure 2B**). We observed higher coefficient values for HHSIs during the pre-induction period (**supplementary Figure 2A**). No other classification patterns reached statistical significance for the pre-induction EEG data (**Figure 2B**). These findings therefore provide further evidence of distinct neural characteristics associated with hypnotic susceptibility in the pre-induction state.

For Δinduction, we found that the classification performance was statistically significant in the alpha and beta frequency ranges (**Figure 2D**; AUC value for alpha-band activity = .55, $p < .05$; AUC value for beta-band activity = .59, $p < .001$). We observed opposite patterns between alpha-band and beta-band clustering coefficients, wherein HHSIs showed more pronounced decrease for the former and increase for the latter following the induction procedure (**Figure 2D**; **supplementary Figure 2**). These findings provide evidence that the induction process yields greater changes in clustering coefficients for individuals with high hypnotic susceptibility compared to those with low hypnotic susceptibility.

Next, we used logistic regression analyses to examine the effects of hypnotic susceptibility on global efficiency and modularity at the network level. Here we included both global efficiency and modularity estimates across broadband frequencies (delta, theta, alpha, beta, gamma) as predictors in our model for predicting hypnotic susceptibility. For the pre-induction EEG data, the logistic regression model (VIFs < 2.8) indicates that global efficiency in delta band activity was a statistically reliable predictor of hypnotic susceptibility (**Figure 2E**). Here, greater global efficiency predicts high hypnotic susceptibility during the pre-induction EEG period (β = 20.16, 95% C.I. [1.3, 39.02]; **Figure 2E**). For Δinduction, the logistic regression model (VIFs < 2.5) revealed that global efficiency in the theta frequencies (β = 18.9, 95% C.I. [.92, 36.99]) and modularity in the delta frequencies (β = -126.01, 95% C.I. [-246.67, -5.35]) were statistically significant predictors (**Figure 2F**). Specifically, the induction procedure was associated with increased global efficiency in the theta frequencies (**Figure 2F**) and decreased modularity (**Figure 2F**) in the delta frequencies in individuals with high hypnotic susceptibility compared to those with low hypnotic susceptibility.

Model comparisons. We used model comparisons to identify the most dominating feature among those we previously identified as statistically significant. Our approach involved systematically evaluating all combinations of statistically significant spectral features and graph theory metrics and then assessing the classification performance of these models. We compared the performance of all models in a pairwise manner using the McNemar test and corrected the p-values for multiple comparisons using the false discovery rate (FDR) method. This approach allowed us to assess which combination of variables provided the best classification performance for each period.

Our results show that the models incorporating the aperiodic exponent consistently outperformed the other models, as indicated by higher AUC values for all these models (**Figure 3A**). The McNemar's Chi-square statistics confirmed the advantage of these models over classification performance (**Supplementary Figure 3A**).

Neural feature ranking. We sought to rank the pertinent neural features by their SVM weights based on the SVM model incorporating all relevant features. Examining feature ranking for all significant features from both the pre-induction period and Δinduction, the model performed above chance-level (AUC value = .69, $p < .001$). Again, the exponent of aperiodic component for the pre-induction resting-state period was the most discriminant feature, followed by the clustering coefficient of alpha-band activity in EEG pertaining to the effect of the induction procedure (**Figure 3B**). Collectively, these analyses highlight the centrality of aperiodic EEG activity for discriminating hypnotic susceptibility.

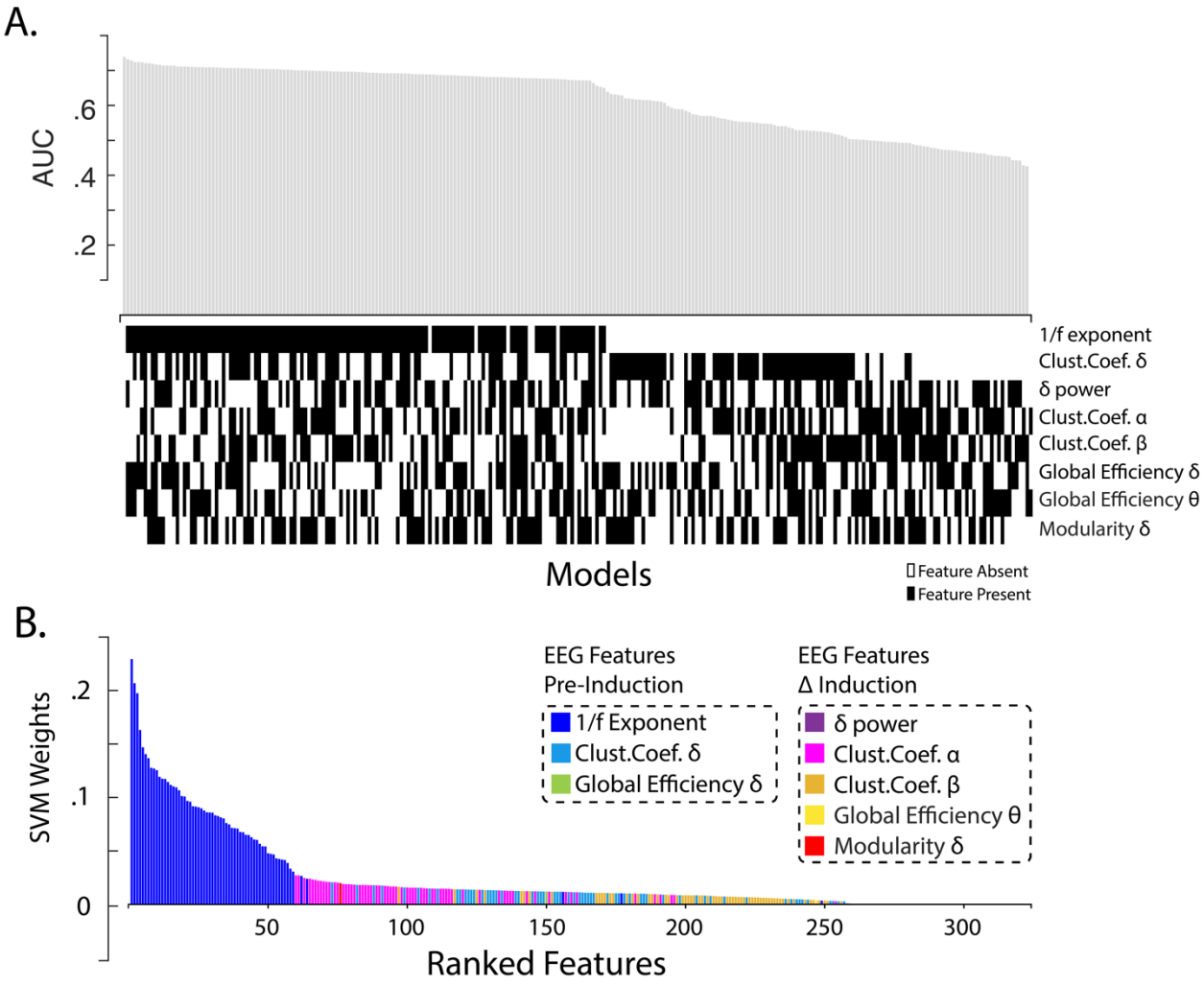

Figure 3. Panel A shows AUC values for each model that were evaluated for the discrimination of high versus low hypnotic susceptible individuals based on neural features from EEG from the pre-induction period and Δinduction. All features had been identified via previous analyses. The x-axis shows the neural features that were included in each model wherein a black square indicates that the neural feature was included in the model, and a white square indicates that the feature was not included in the model. Weights of SVM classifiers trained to differentiate high and low hypnotic susceptibility using EEG features from both pre-induction EEG period and Δinduction. Features were identified in preceding analyses. The x-axis ranks neural features in descending order, while the y-axis displays the absolute values of the SVM weights.

Discussion

The current study provides a comprehensive investigation into the neural correlates of an individual's receptiveness to hypnotic suggestion. Our findings confirmed that the neural basis of hypnotic susceptibility is complex and multifaceted. Remarkably, we observed that an individual's hypnotic susceptibility can be predicted from their ongoing brain data recorded before hypnotic induction, principally from the aperiodic component of brain activity. These findings complement earlier observations from functional neuroimaging studies (39, 40), and provide an electrophysiological account for

the intriguing observation that susceptibility to hypnotic suggestion is a predisposition that varies across the general population.

Our findings suggest that the neural responses to hypnotic induction differed across HHSIs and LHSIs across several frequency bands. In particular, we found that rhythmic delta band activity distinguishes between individuals low and high on hypnotic susceptibility. These results diverge from recent studies that found no differences in spectral power across varying levels of hypnotic susceptibility (41). We attribute this discrepancy to dissimilarities in methodology: We controlled for the contribution of aperiodic brain activity which represents an important component of hypnotic phenomena.

Recent work suggests that hypnotic induction induces polyrhythmic changes in network topology (20). At the psychological level, the induction procedure is associated with increased mental absorption, feelings of relaxation, and preparation for hypnotic responding (42). The effects we observed relative to modifications in network topologies are therefore likely indicative of the differential expression of these mental states across HHSIs and LHSIs. Interestingly, analogous shifts in network structures across delta, alpha, and beta frequencies have also been observed when comparing neural patterns of novice and expert meditators (43, 44). This observation resonates with the hypothesis suggesting a convergence between hypnosis and meditative practices (45). Indeed, both practices encompass the involvement of attention resources and the recruitment of overlapping brain networks (46, 47).

Critically, our results revealed that the aperiodic component of brain activity at baseline (the pre-induction period) stands out as the primary neural feature that contributes most to the classification (**Figures 3**). This outcome supports the idea that hypnotic susceptibility reflects a cerebral predisposition and brings about the possibility of assessing it using EEG at baseline instead of using standardized protocols (48). To some degree, these finding challenges traditional expectations in EEG-based hypnosis research. Based on previous work, some would argue that that the principal neural signature underlying hypnotic susceptibility should manifest following hypnotic induction (e.g., 49). This expectation is reinforced by work reporting modifications of both oscillatory activity and long-range temporal correlations (a scale-free quantitative assessment of amplitude fluctuations in the signal that relates to the aperiodic component of the EEG) in response to hypnotic induction (12, 13, 18). We note that participants were not blind to the experimental manipulation, which entails that our findings likely include effects of expectations (50). Mounting evidence proposes that ability for hypnotic responding is best captured by interrelated components characterized by a structure comprising a core ability that superordinate secondary ones (22). One may conjecture that the centrality of the aperiodic slope for differentiating HHISs and LHSIs during the pre-induction period reflects this core component.

Not only do our results confirm the importance of probing the aperiodic component of brain activity (28), but they also indicate that the properties of this aperiodic component are actually central to the mechanisms of hypnotic phenomena. This result also

contributes to mounting evidence linking the aperiodic activity of EEG to inter-individual differences across various research areas within psychology (30, 51).

Previous work highlights how differences in spectral power between LHSIs and HHSIs can index differences in cognitive abilities, such as mental imagery (52). Evidence from topological analysis of the EEG signal comparing visual perception and visual imagery supports this viewpoint (53). However, rather than indicate posterior regions of the cortex, the more anterior topographical pattern of classifier's features (**Figure 2A**) instead aligns more closely with research positing that the predisposition for efficient hypnotic responding is related with prefrontal cortex (PFC) activity (Cojan et al., 2015; Hoeft et al., 2012). In particular, findings show that stimulation of the dorsolateral PFC using transcranial magnetic stimulation increases susceptibility to hypnosis (54, 55). One may speculate that differences in PFC activity as function of hypnotic susceptibility relates to fluctuations in executive functions (56-58), phenomenological control (59) or metacognitive processing (60). However, links between the aperiodic component in EEG recordings and executive functions has yet to be thoroughly investigated. While research on the aperiodic component is largely nascent (28), emerging evidence reveals that cognitive impairments, including shifts in executive functioning, are associated with a shallower slope of the aperiodic component (61). Prevailing views propose that the slope of the aperiodic exponent indexes balance between excitatory and inhibitory activities of neural populations (62, 63). In this framework, a flatter aperiodic exponent corresponds to a greater excitation-inhibition ratio, which entails lower inhibition of cortical circuits and greater neuronal noise decoupled from oscillatory (synchronized). Prevailing views link such departure from inhibition and greater neuronal noise to poorer cognitive performance (64). In this regard, at least one study lends support to the notion that baseline cortical excitability represents a neural characteristic of hypnotic susceptibility (65). Therefore, greater slope values in HHSIs relative to LHSIs might reflect differences in executive control and cognitive control abilities associated with differences in neuronal excitability. These findings underscore the importance of pursuing further research that specifically examines the relationship between hypnotic susceptibility differences and the aperiodic component.

In conclusion, our research offers novel perspectives on the neural foundations of hypnotic susceptibility, and enriches the growing body of scientific literature highlighting the critical role of the aperiodic component in EEG signals for deciphering the nuances of neural differences between individuals (66-70). Taken together, the outcome of our data-driven approach corroborates the idea that the hypnotic states, and our susceptibility to hypnotic suggestion, are mediated by several diverse electrophysiological components (23). A surprising finding was the prominence of the slope of the aperiodic EEG activity in the pre-induction phase as the key neural feature. This observation supports the view that baseline brain activity offers an accurate representation of an individual's susceptibility to hypnosis. Our findings pave the way for further research into the contribution of the aperiodic slope to the neural mechanisms that underlie hypnotic experiences, and more generally they demonstrate the feasibility of developing novel approaches to assess hypnotic susceptibility based on physiological recordings. Indeed, with the growing focus on the clinical use of hypnosis, it's crucial to delve deeper into the

variations in hypnotic response among individuals. This understanding is key to enhancing the effectiveness of clinical hypnosis within the framework of personalized medicine.

Methods

Participants. Our recruitment procedure comprised two stages. First, potential participants were invited to a pre-screening session, during which we assessed their hypnotic susceptibility using the Harvard Group Scale of Hypnotic Susceptibility, Form A (HGSHS:A; 71). Subsequently, we selected 75 individuals from this initial pool to undergo EEG recordings. For the present study, we focused on neural activity data from 40 individuals (27 females, mean age of 21.98 y.o. (st.dev. = 4.41)) based on their HGSHS:A scores. Specifically, we included individuals who scored above 8, indicating high hypnotic susceptibility (HHSIs), and individuals who scored below 4, indicating low hypnotic susceptibility (LHSIs). This work aligns with previous studies focusing on high and low hypnotic susceptible individuals to maximize the detection of the effect. We Participants were not informed of their scores. Participants who completed the second part of our recruitment procedure received monetary compensation. All study procedures were approved by the local institutional review board. Participants provided written consent.

Our sample size was determined based on prior research investigating the impact of hypnotic susceptibility on spectral features and connectivity measures during EEG, which reported statistically significant findings. See Supplemental Materials.

Procedure. The assessment of hypnotic susceptibility was conducted following the standard procedure of the HGSHS:A in a separate experimental session on a different day. The experimental procedure consisted of a 5-minute EEG that was recorded at baseline (i.e., pre-induction period), followed by the hypnotic induction procedure, and subsequently, another 5-minute EEG recording.

During the EEG recording, participants were seated in a quiet and dimly lit room. The experimenter, who conducted the induction procedure, positioned themselves approximately one meter behind the participants throughout the experiment. We recorded the baseline EEG for all participants before the induction-related EEG, instead of counterbalancing our experimental conditions. This approach prevented contamination (i.e., carry-over effects) of the baseline period by the hypnotic induction, as it is challenging to determine the duration required for the effects of hypnosis to wash out after the de-induction. Additionally, since the objective of the current study was to differentiate highly hypnotic susceptible individuals from those with low susceptibility, the order of the baseline and induction-related EEG recordings was deemed irrelevant.

During the baseline recording, participants were instructed by the experimenter to close their eyes while remaining vigilant. For the induction period, the experimenter read a script (see supplementary material), which included instructions for participants to close their eyes, and the 5-minute EEG recording was conducted after the completion of the induction.

Electroencephalography. We recorded EEG signals using 64 Ag/AgCl active electrodes at a sampling rate of 1000 Hz (ActiCap System; Brain Products GmbH; Gilching, Germany). We positioned additional bipolar electrodes at the outer canthi, as well as the superior and inferior orbits of the left eye. We kept impedances of all electrodes below 10 kΩ, while all electrophysiological signals were amplified (ActiChamp System; BrainPProducts GmbH; Gilching, Germany). Electrode impedences were kept below 10 kΩ. Data was collected online at 1000Hz and down sampled to 250Hz offline for data analysis. Data acquisition was done via Brain Recorder (Brain Products Inc., GmbH) while pre-processing and data analysis were completed through Brain Vision Analyzer, Brainstorm (72), and custom MATLAB scripts (version R2022A; MathWorks Inc, MA). Bad electrodes were topographically interpolated using spherical splines (< 3% electrodes). EEG recordings were re-referenced to the average of all EEG electrodes offline. All EEG data were inspected for muscle-related, eye movement or technical artifacts, which were removed before continuing the analysis.

Spectral features. Spectral features were computed individually for each channel using the *specparam* algorithm for spectral parametrization as implemented in Brainstorm (Figure 1A; 72, 73). The *specparam* algorithm decomposes power spectra into periodic and aperiodic (1/f-like) components by fitting the power spectral density in log-log space. The periodic component is characterized by the center frequency, bandwidth, and relative amplitude of the oscillatory peak, while the aperiodic component is defined by the offset and slope of the power spectrum density. In our analysis, we employed the model-selection implementation of specparam to fit the power spectral density from 1 to 40Hz, considering up to 6 peaks, with a minimum peak height of 1db, a peak threshold of 2, a proximity threshold of 0.75, peak width limits between 0.5 to 12 Hz, and a fixed aperiodic mode. Goodness-of-fit was evaluated based on mean-square error, and no significant differences were observed between high and low hypnotic susceptible individuals for the pre-induction period and Δ induction. Specifically, AUC for classification was .51 ($p > .5$) for pre-induction EEG and .49 (for Δinduction on EEG using the multivariate pattern classification described below. We then extracted the power spectrum values for the periodic component of each EEG channel by subtracting the aperiodic component from the power spectrum density. Finally, we calculated the average spectrum values separately for delta (1 to 3.5Hz), theta (4 to 7.5Hz), alpha (8 to 13.5Hz), and beta (14 to 39Hz) broadband frequencies. In summary, our analysis encompassed six spectral features: the offset and slope of the aperiodic component, as well as corrected power for delta, theta, alpha, and beta oscillations.

Features of network topology. To extract network topology features, we utilized graph theory metrics on sensor-level connectivity patterns, employing the Brain Connectivity Toolbox (Figure 1B; 74). Initially, we applied the Hilbert transformation to filter the EEG data at specific frequency bands, namely delta (1 to 3.5Hz), theta (4 to 7.5Hz), alpha (8 to 13.5Hz), beta (14 to 39Hz), and gamma (30 to 50Hz) frequencies. Subsequently, we estimated functional connectivity between all electrode pairs using wPLI to account for volume conduction effects on brain connectivity estimation (38). Then, we opted to normalize the edges into weights ranging from 0 to 1 rather than converting the 64 by 64 functional network into sparse and binarized patterns (37). This approach ensured the

preservation of valuable information without loss due to subjective thresholding choices. From these weighted undirected connectivity matrices, we extracted three distinct graph measures for all frequency bands: The clustering coefficient, derived from the geometric mean of local triangle configurations associated with each node, which provides insight into the extent of node clustering (75); global efficiency, measured as the inverse of the shortest path length, that quantifies the level of shared information across the entire network (76); and global modularity to estimate the degree to which networks are divided into communities (77). These graph theory metrics allowed us to evaluate network integration and segregation as a function of hypnotic induction and susceptibility to hypnotic suggestions. Our graph theoretical approach therefore yielded three separate neural features, clustering coefficient, global efficiency and global modularity across all broad frequency bands.

Multivariate pattern analysis and leave-one-out cross-validation. We employed a multivariate pattern analysis combined with a leave-one-out cross-validation strategy to train and test linear support vector machine (SVM) models. The objective was to discriminate between high and low hypnotic susceptible individuals based on spectral and network topological features (**Figure 1C**). To minimize classification biases, we carefully balanced the classes in our training set, including 16 high and 16 low hypnotic susceptible individuals in each iteration (78). In each iteration of the cross-validation process, one participant was left out for testing the SVM model, while we randomly selected 16 participants from each class for the training set. This procedure was repeated to ensure that each participant served as a test case 10 times for comprehensive cross-validation. The SVM linear model was trained using the 64 EEG channels as features for classification. We assessed the classification performance using the area under the curve (AUC).

The observed classification performance was compared to a surrogate distribution generated from 1000 random permutations. In each permutation, the class labels were randomly shuffled during the training process (79). Statistical significance was set at alpha = .05. The observed classification performance was considered statistically significant only if it outperformed 95% the performance of the upper-part (i.e., one-tail) surrogate distribution.

To facilitate interpretation, we further transformed the weights of the SVM classifiers based on the covariance of the training dataset (80). These transformed weights were then averaged across all training iterations. We also extracted PSD and graph theoretical values for the channels where we observed the top 5% SVM weights to better understand how hypnotic susceptibility and the induction procedure impacted EEG.

We evaluated spectral features and clustering coefficients for pre-induction and Δinduction separately.

In addition to EEG, we applied our multivariate classification approach to vertical and horizontal electro-oculogram signals (VEOG and HEOG) to determine whether we could discriminate between HHSIs and LHSIs across both pre-induction and Δinduction

separately. This classification procedure showed that we could not discriminate between HHSIs and LHSIs based on signals from eye movements.

Feature comparisons. The previous analyses allowed us to identify spectral and network features from the pre-induction and Δinduction EEG that differentiate between high and low hypnotic susceptible individuals on their own. Next, we aimed to ascertain the top discriminant feature when we combine them. Our approach was twofold.

First, we used model comparisons. Using the previously described multivariate pattern classification analysis and leave-one-out cross-validation approach, we trained and tested SVM models that incorporated all possible combinations of features we previously identified as statistically significant on their own. This assessment was performed three times: once for the pre-induction EEG period, then for Δinduction EEG data, and thirdly for all possible combinations of significant features from both the pre-induction EEG and Δinduction. For each model, we calculated the AUC as a measure of classification performance. To compare the classification performance of all models, we utilized McNemar's test (81), which is a reliable method for comparing classification performances based on contingency tables (82). To account for multiple comparisons, we corrected the p-values from these tests using the false discovery rate correction method proposed by Benjamini and Hochberg (1995).

Second, we used feature ranking. Here included all significant features into SVM models and then ranked the absolute value of the SVM weights following the procedure from Haufe et al. (80) described earlier. We applied this feature ranking procedure three times: once for all significant features from the pre-induction EEG, second for all significant features for Δinduction, and thirdly for significant features from both the pre-induction and Δinduction EEG.

References

1. D. B. Terhune, A. Cleeremans, A. Raz, S. J. Lynn, Hypnosis and top-down regulation of consciousness. *Neuroscience & Biobehavioral Reviews* (2017).
2. R. J. Pekala, Hypnosis as a "state of consciousness": How quantifying the mind can help us better understand hypnosis. *American Journal of Clinical Hypnosis* **57**, 402-424 (2015).
3. P. Rainville, D. D. Price, Hypnosis phenomenology and the neurobiology of consciousness. *International Journal of Clinical and Experimental Hypnosis* **51**, 105-129 (2003).
4. C. Timmermann *et al.*, A neurophenomenological approach to non-ordinary states of consciousness: hypnosis, meditation, and psychedelics. *Trends in Cognitive Sciences* **27**, 139-159 (2023).
5. A. M. Weitzenhoffer, Hypnotic susceptibility revisited. *American Journal of Clinical Hypnosis* **22**, 130-146 (1980).
6. P. Rainville, G. H. Duncan, D. D. Price, B. Carrier, M. C. Bushnell, Pain affect encoded in human anterior cingulate but not somatosensory cortex. *Science* **277**, 968-971 (1997).
7. E. Cardeña, The phenomenology of deep hypnosis: Quiescent and physically active. *International Journal of Clinical and Experimental Hypnosis* **53**, 37-59 (2005).
8. M. R. Nash, A. J. Barnier, *The Oxford handbook of hypnosis : theory, research and practice* (Oxford University Press, New York, 2008), pp. ix, 791 p.
9. P. Rainville *et al.*, Hypnotic automaticity in the brain at rest: An arterial spin labelling study. *International Journal of Clinical and Experimental Hypnosis* **67**, 512-542 (2019).
10. C. Desmarteaux *et al.*, Brain responses to hypnotic verbal suggestions predict pain modulation. *Frontiers in Pain Research* **2**, 757384 (2021).
11. M. Landry, M. Lifshitz, A. Raz, Brain correlates of hypnosis: A systematic review and meta-analytic exploration. *Neuroscience & Biobehavioral Reviews* **81**, 75-98 (2017).
12. A. Vanhaudenhuyse, S. Laureys, M. E. Faymonville, Neurophysiology of hypnosis. *Neurophysiologie Clinique/Clinical Neurophysiology* **44**, 343-353 (2014).
13. V. De Pascalis, EEG Oscillations and Neural Functional Connectivity Underpinning Hypnosis and Hypnotizability. *Preprints* 10.20944/preprints202312.0382.v1 (2023).
14. V. De Pascalis, E. L. Santarcangelo, Hypnotizability-Related Asymmetries: A Review.
15. E. Malloggi, E. L. Santarcangelo, Physiological Correlates of Hypnotizability: Hypnotic Behaviour and Prognostic Role in Medicine. *Brain Sciences* **13**, 1632 (2023).
16. V. De Pascalis, P. M. Penna, 40-Hz Eeg Activity During Hypnotic Induction and Hypnotic Testing. *International Journal of Clinical and Experimental Hypnosis* **38**, 125-138 (1990).
17. D. Spiegel, S. Cutcomb, C. Ren, K. Pribram, Hypnotic hallucination alters evoked potentials. *Journal of Abnormal Psychology* **94**, 249 (1985).

18. J.-S. Lee *et al.*, Fractal analysis of EEG in hypnosis and its relationship with hypnotizability. *Intl. Journal of Clinical and Experimental Hypnosis* **55**, 14-31 (2007).
19. G. A. Jamieson, A. P. Burgess, Hypnotic induction is followed by state-like changes in the organization of EEG functional connectivity in the theta and beta frequency bands in high-hypnotically susceptible individuals. *Frontiers in human neuroscience* **8**, 528 (2014).
20. R. Panda *et al.*, Altered Brain Connectivity and Network Topological Organization in a Non-ordinary State of Consciousness Induced by Hypnosis. *Journal of Cognitive Neuroscience* **35**, 1394-1409 (2023).
21. M. E. Sabourin, S. D. Cutcomb, H. J. Crawford, K. Pribram, EEG correlates of hypnotic susceptibility and hypnotic trance: Spectral analysis and coherence. *International journal of psychophysiology* **10**, 125-142 (1990).
22. A. J. Barnier, D. B. Terhune, V. Polito, E. Z. Woody, A componential approach to individual differences in hypnotizability. *Psychology of Consciousness: Theory, Research, and Practice* **9**, 130 (2022).
23. M. Landry, P. Rainville, "Beyond the neural signature of hypnosis: Neuroimaging studies support a multifaceted view of hypnotic phenomena" in Routledge International Handbook of Clinical Hypnosis*,* J. Linden, L. Sugerman, G. de Benedittis, K. Varga, Eds. (Taylor & Francis, London, 2024).
24. M. Landry, A. Raz, Hypnosis and imaging of the living brain. *American Journal of Clinical Hypnosis* **57**, 285-313 (2015).
25. J.-R. Laurence, D. Beaulieu-Prévost, T. Du Chéné, "Measuring and understanding individual differences in hypnotizability" in The Oxford Handbook of Hypnosis: Theory, Research, and Practice*,* A. J. Barnier, M. R. Nash, Eds. (Oxford University Press, New York, 2008).
26. A. J. Barnier, R. E. Cox, K. M. McConkey, The Province of "Highs": The High Hypnotizable Person in the Science of Hypnosis and in Psychological Science. *Psychology of Consciousness: Theory, Research, and Practice* **1**, 168-183 (2014).
27. M. D. Yapko, *Essentials of hypnosis* (Routledge, New York, ed. 2nd, 2015).
28. T. Donoghue, N. Schaworonkow, B. Voytek, Methodological considerations for studying neural oscillations. *European Journal of Neuroscience* **55**, 3502-3527 (2022).
29. L. E. Wilson, J. da Silva Castanheira, S. Baillet, Time-resolved parameterization of aperiodic and periodic brain activity. *eLife* **11**, e77348 (2022).
30. M. Gerster *et al.*, Separating neural oscillations from aperiodic 1/f activity: challenges and recommendations. *Neuroinformatics*, 1-22 (2022).
31. F. Lopes da Silva, EEG and MEG: Relevance to Neuroscience. *Neuron* **80**, 1112-1128 (2013).
32. B. J. He, Scale-free brain activity: past, present, and future. *Trends in Cognitive Sciences* **18**, 480-487 (2014).
33. C. Maschke, C. Duclos, A. M. Owen, K. Jerbi, S. Blain-Moraes, Aperiodic brain activity and response to anesthesia vary in disorders of consciousness. *NeuroImage* **275**, 120154 (2023).

34. L. Pei, X. Zhou, F. K. S. Leung, G. Ouyang, Differential associations between scale-free neural dynamics and different levels of cognitive ability. *Psychophysiology* **60**, e14259 (2023).
35. M. Gyurkovics, G. M. Clements, K. A. Low, M. Fabiani, G. Gratton, Stimulus-induced changes in 1/f-like background activity in EEG. *Journal of Neuroscience* **42**, 7144-7151 (2022).
36. E. Bullmore, O. Sporns, Complex brain networks: graph theoretical analysis of structural and functional systems. *Nature Reviews Neuroscience* **10**, 186-198 (2009).
37. M. Rubinov, O. Sporns, Weight-conserving characterization of complex functional brain networks. *Neuroimage* **56**, 2068-2079 (2011).
38. M. Vinck, R. Oostenveld, M. van Wingerden, F. Battaglia, C. M. A. Pennartz, An improved index of phase-synchronization for electrophysiological data in the presence of volume-conduction, noise and sample-size bias. *Neuroimage* **55**, 1548-1565 (2011).
39. F. Hoeft *et al.*, Functional brain basis of hypnotizability. *Archives of General Psychiatry* **69**, 1064-1072 (2012).
40. A. Huber, F. Lui, D. Duzzi, G. Pagnoni, C. A. Porro, Structural and Functional Cerebral Correlates of Hypnotic Suggestibility. *PloS one* **9**, e93187 (2014).
41. G. Rho *et al.*, Linear and Nonlinear Quantitative EEG Analysis during Neutral Hypnosis following an Opened/Closed Eye Paradigm.
42. D. B. Terhune, E. Cardeña, Nuances and Uncertainties Regarding Hypnotic Inductions: Toward a Theoretically Informed Praxis. *American Journal of Clinical Hypnosis* **59**, 155-174 (2016).
43. R. van Lutterveld *et al.*, Meditation is associated with increased brain network integration. *NeuroImage* **158**, 18-25 (2017).
44. A. Lardone *et al.*, Topological changes of brain network during mindfulness meditation: an exploratory source level magnetoencephalographic study. *AIMS Neuroscience* **9**, 250-263 (2022).
45. A. Raz, M. Lifshitz, *Hypnosis and meditation: Towards an integrative science of conscious planes* (Oxford University Press, Oxford, UK, 2016).
46. M. Landry, A. Raz, Heightened states of attention: From mental performance to altered states of consciousness and contemplative practices. *Intellectica* **66**, 139-159 (2016).
47. M. Lifshitz, M. van Elk, T. M. Luhrmann, Absorption and spiritual experience: A review of evidence and potential mechanisms. *Consciousness and Cognition* **73**, 102760 (2019).
48. G. Baghdadi, A. M. Nasrabadi, Comparison of different EEG features in estimation of hypnosis susceptibility level. *Computers in biology and medicine* **42**, 590-597 (2012).
49. D. B. Terhune, E. Cardeña, M. Lindgren, Differential frontal-parietal phase synchrony during hypnosis as a function of hypnotic suggestibility. *Psychophysiology* **48**, 1444-1447 (2011).
50. B. Gandhi, D. A. Oakley, Does 'hypnosis' by any other name smell as sweet? The efficacy of 'hypnotic'inductions depends on the label 'hypnosis'. *Consciousness and Cognition* **14**, 304-315 (2005).

51. S. M. Pani, L. Saba, M. Fraschini, Clinical applications of EEG power spectra aperiodic component analysis: A mini-review. *Clinical Neurophysiology* (2022).
52. F. I. Cavallaro *et al.*, Hypnotizability-related EEG alpha and theta activities during visual and somesthetic imageries. *Neuroscience Letters* **470**, 13-18 (2010).
53. E. Ibáñez-Marcelo, L. Campioni, A. Phinyomark, G. Petri, E. L. Santarcangelo, Topology highlights mesoscopic functional equivalence between imagery and perception: The case of hypnotizability. *NeuroImage* **200**, 437-449 (2019).
54. Z. Dienes, S. Hutton, Understanding hypnosis metacognitively: rTMS applied to left DLPFC increases hypnotic suggestibility. *Cortex* **49**, 386-392 (2013).
55. A. Faerman *et al.*, Stanford Hypnosis Integrated with Functional Connectivity-targeted Transcranial Stimulation (SHIFT): a preregistered randomized controlled trial. *Nature Mental Health* **2**, 96-103 (2024).
56. B. A. Parris, The role of frontal executive functions in hypnosis and hypnotic suggestibility. *Psychology of Consciousness: Theory, Research, and Practice* **4**, 211-229 (2017).
57. A. Faerman, D. Spiegel, Shared cognitive mechanisms of hypnotizability with executive functioning and information salience. *Scientific Reports* **11**, 5704 (2021).
58. T. Egner, A. Raz, "Cognitive Control Processes and Hypnosis" in Hypnosis and Conscious States: The cognitive neuroscience perspective*,* G. A. Jamieson, Ed. (Oxford University Press, New York, NY, 2007), pp. 29-50.
59. Z. Dienes, P. Lush, The Role of Phenomenological Control in Experience. *Current Directions in Psychological Science* **32**, 145-151 (2023).
60. P. Lush, P. Naish, Z. Dienes, Metacognition of intentions in mindfulness and hypnosis. *Neuroscience of Consciousness* **2016** (2016).
61. A. J. Finley *et al.*, Resting EEG Periodic and Aperiodic Components Predict Cognitive Decline Over 10 Years. *bioRxiv*, 2023-2007 (2023).
62. R. Gao, E. J. Peterson, B. Voytek, Inferring synaptic excitation/inhibition balance from field potentials. *Neuroimage* **158**, 70-78 (2017).
63. L. Waschke *et al.*, Modality-specific tracking of attention and sensory statistics in the human electrophysiological spectral exponent. *Elife* **10**, e70068 (2021).
64. B. Voytek, R. T. Knight, Dynamic network communication as a unifying neural basis for cognition, development, aging, and disease. *Biological psychiatry* **77**, 1089-1097 (2015).
65. V. Spina, C. Chisari, E. L. Santarcangelo, High motor cortex excitability in highly hypnotizable individuals: a favourable factor for neuroplasticity? *Neuroscience* **430**, 125-130 (2020).
66. M. A. Immink *et al.*, Resting-state aperiodic neural dynamics predict individual differences in visuomotor performance and learning. *Human Movement Science* **78**, 102829 (2021).
67. R. Bódizs *et al.*, A set of composite, non-redundant EEG measures of NREM sleep based on the power law scaling of the Fourier spectrum. *Scientific reports* **11**, 2041 (2021).
68. N. Schaworonkow, B. Voytek, Longitudinal changes in aperiodic and periodic activity in electrophysiological recordings in the first seven months of life. *Developmental cognitive neuroscience* **47**, 100895 (2021).

69. L. Waschke, M. Wöstmann, J. Obleser, States and traits of neural irregularity in the age-varying human brain. *Scientific Reports* **7**, 17381 (2017).
70. D. Cellier, J. Riddle, I. Petersen, K. Hwang, The development of theta and alpha neural oscillations from ages 3 to 24 years. *Developmental Cognitive Neuroscience* **50**, 100969 (2021).
71. R. E. Shor, E. C. Orne, *Harvard group scale of hypnotic susceptibility, Form: A* (Consulting psychologists press, Palo Alto, CA, 1962).
72. F. Tadel, S. Baillet, J. C. Mosher, D. Pantazis, R. M. Leahy, Brainstorm: a user-friendly application for MEG/EEG analysis. *Computational intelligence and neuroscience* **2011**, 8 (2011).
73. T. Donoghue *et al.*, Parameterizing neural power spectra into periodic and aperiodic components. *Nature Neuroscience* **23**, 1655-1665 (2020).
74. M. Rubinov, O. Sporns, Complex network measures of brain connectivity: uses and interpretations. *Neuroimage* **52**, 1059-1069 (2010).
75. J.-P. Onnela, J. Saramäki, J. Kertész, K. Kaski, Intensity and coherence of motifs in weighted complex networks. *Physical Review E* **71**, 065103 (2005).
76. V. Latora, M. Marchiori, Efficient Behavior of Small-World Networks. *Physical Review Letters* **87**, 198701 (2001).
77. M. E. Newman, Modularity and community structure in networks. *Proceedings of the national academy of sciences* **103**, 8577-8582 (2006).
78. P. Thölke *et al.*, Class imbalance should not throw you off balance: Choosing the right classifiers and performance metrics for brain decoding with imbalanced data. *bioRxiv*, 2022-2007 (2022).
79. E. Combrisson, K. Jerbi, Exceeding chance level by chance: The caveat of theoretical chance levels in brain signal classification and statistical assessment of decoding accuracy. *Journal of Neuroscience Methods* **250**, 126-136 (2015).
80. S. Haufe *et al.*, On the interpretation of weight vectors of linear models in multivariate neuroimaging. *Neuroimage* **87**, 96-110 (2014).
81. Q. McNemar, Note on the sampling error of the difference between correlated proportions or percentages. *Psychometrika* **12**, 153-157 (1947).
82. T. G. Dietterich, Approximate statistical tests for comparing supervised classification learning algorithms. *Neural computation* **10**, 1895-1923 (1998).

SUPPLEMENTARY MATERIAL

We present values derived from spectral features and graph theoretical clustering coefficients, which are based on wPLI connectivity patterns. Following our comprehensive multivariate pattern analysis, three EEG channels were strategically selected for each neural feature where we were able to classify hypnotic susceptibility better than chance level. We detail the values for these channels during both the pre-induction and post-induction periods, as well as the differential values between these two states. Values are presented separately for LHSIs and HHSIs. Consequently, this illustration facilitates the tracking of variations across different conditions, thereby providing a deeper insight into the implications and effectiveness of our classification procedure.

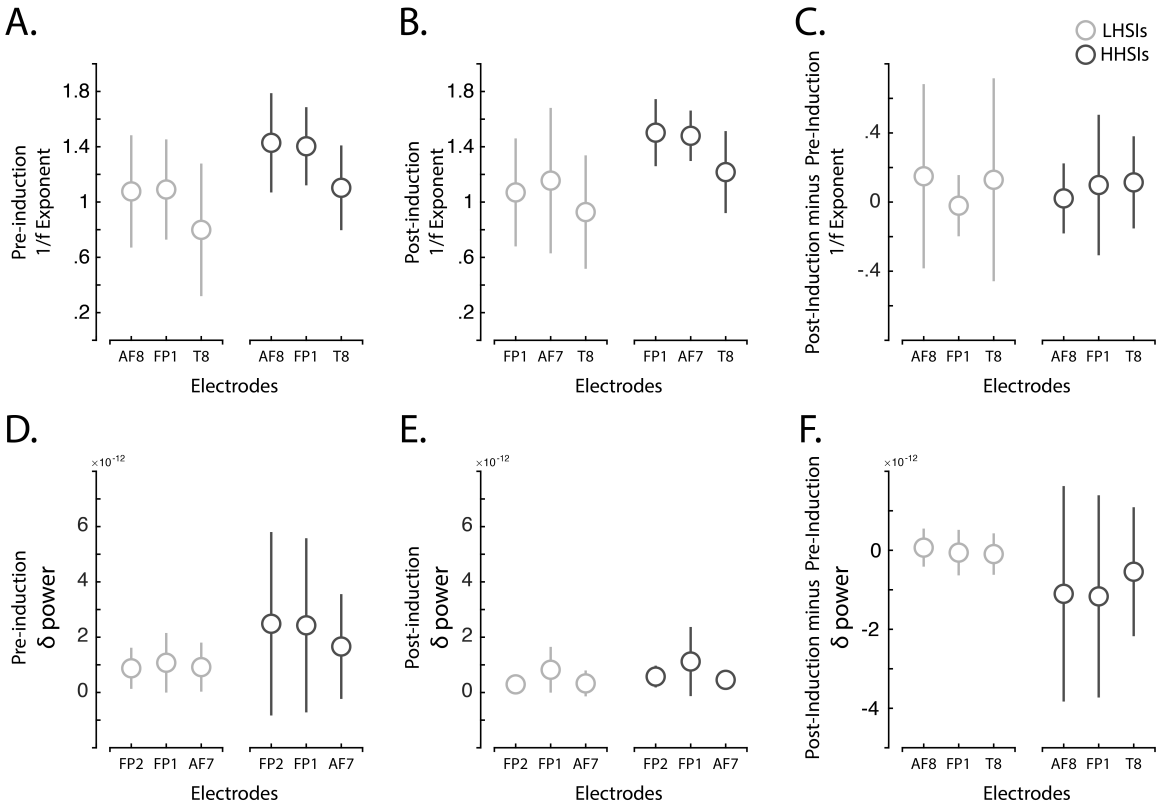

Supplementary Figure 1. Estimations of exponent slope values for channels AF8, FP1, and T8 across Low Hypnotic Susceptibility Individuals (LHSIs) and High Hypnotic Susceptibility Individuals (HHSIs). Panel A illustrates these estimates for the pre-induction period, Panel B for the post-induction period, and Panel C details the variance between these two conditions. Additionally, the figure presents spectral power data for broadband delta frequencies in channels FP2, FP1, and AF7. This data is also segmented across LHSIs and HHSIs, with Panel D showing the pre-induction period, Panel E the post-induction period, and Panel F highlighting the differences between these conditions.

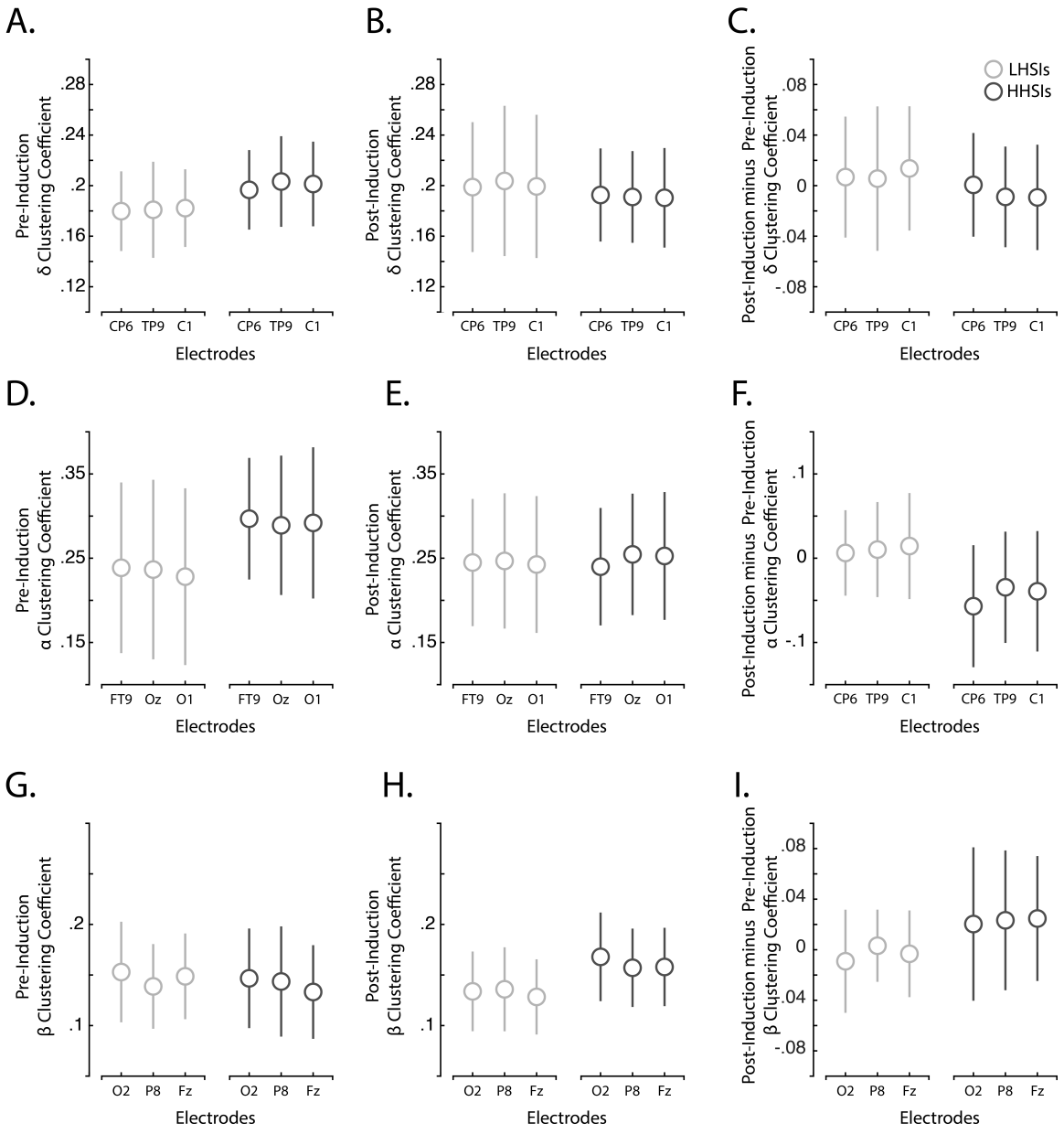

Supplementary Figure 2. Estimations of clustering coefficients across delta (panels A, B, C; channels CP6, TP9, and C1), alpha (panels D, E, F; channels FT9, Oz, and O1), and beta (panels G, H, I; channels O2, P8, and Fz) frequencies across Low Hypnotic Susceptibility Individuals (LHSIs) and High Hypnotic Susceptibility Individuals (HHSIs). Panels A, D, and G correspond to the pre-induction period, panels B, E and H the post-induction period, and Panel C, F and I indicate the differences between these conditions.

We used model comparison to identify the top feature for predicting hypnotic susceptibility. We used McNemar's chi-square statistics to compare the performance of models (**Supplementary figure 3**).

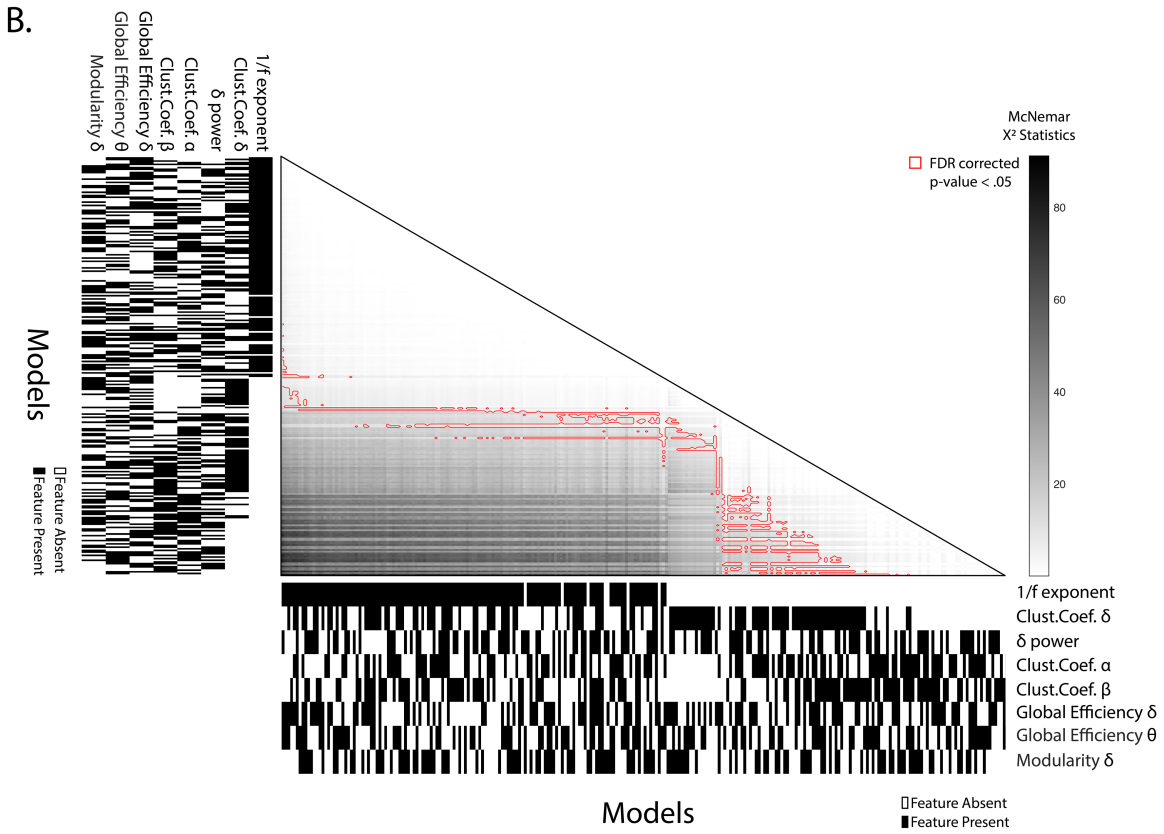

Supplementary Figure 3. Panel A shows the corresponding McNemar's Chi-square statistics where we compared all models in a pairwise manner. Red contours indicate statistically significant comparisons after FDR corrections for multiple comparisons.

Next, here is the script we used for the hypnotic induction across all participants.

Hypnotic Induction Script

Alright, let's begin.

Right now, there is nothing to do at all.
Your mind might start to wander…
You might feel the chair below you, or the EEG cap on your head…
and as you notice these sensations...
you might find yourself noticing the sound of my voice…
and as you notice the sound of my voice...
or notice your sensations…
You may also begin to become aware of how easy it would be to close your eyes right now…
And as you begin to wonder what it would feel like to close your eyes now…
As you continue to notice the sound of my voice…
your eyelids might feel heavy…
Or perhaps they might just feel tired…
I don't know to what extent your eyelids might feel heavy or tired…

However they feel, these sensations might make you want to just
close your eyes….
Perhaps you can imagine heavy eyes, tired eyes…
and as you notice this...
it may feel nice to just let them rest.
And as you let your eyes rest now, you might imagine that you are already developing the capacity to enter a very deep state, now…
And as my voice continues, you may also become aware of your breathing…
In-breath, and out-breath
Perhaps you can imagine that with each out-breath, you go deeper and deeper ... more relaxed, more deep
And with each out-breath you may notice yourself going deeper now (time with outbreaths)
That's right
Perhaps you feel relaxed right now...
perhaps you feel heavy…
Perhaps you feel in a deep, deep state...
Anyway you feel right now is exactly right
And as you are aware of how you feel,
Deep, tired, heavy…
as you become aware of how you feel..
you might notice you also grow more aware of your capacity to enter a very deep state…
Somehow this might remind you of other capacities you have to enter different mental states….
perhaps this might remind you of a specific mental state….
A time when you couldn't read…
Maybe this might be when looking at words in another language…
Or perhaps this might remind you of when you were a child, before you learned to read....
And as you remember this… you might notice that written words begin to change in your minds eye…
Perhaps they simply look 'off', strange…
Or perhaps they appear to be written in a foreign language…
However written words change for you now is perfectly fine...
As my voice continues…
You might notice your relationship to written words continues to change…
so that words might become completely illegible....
you might imagine that if you saw a written word in front of you…
You might not be able to read it…
and perhaps as you imagine being completely unable to read words in front of you…
You might notice that other abilities are preserved….
Numbers in numerical form are completely legible…
And as you continue to notice how strange and illegible written words appear,
You might grow increasingly aware of how clear and legible numbers are.

And you might notice the contrast between numbers that are spelled out…
that might be blurry, illegible, confusing, nonsensical...
And numbers that appear in numerical form…
clear, crystal clear...
And you can just allow this process to naturally happen…
you can rest assured that your body and mind
Know how to do that for you …
And will continue to do so now…
And just allow this experience to happen…
you can simply allow the experience of being unable to read words arise …
However it may arise…
That's right…
As my voice continues…
You may notice how deep your mental state is...
and as you notice this...
you might notice your capacity to change how you read deepen…
That's right.

So now we will begin the first task.